The Plant Cell, Vol. 29: 331–344, February 2017, www.plantcell.org

Molecular Profiles of Contrasting Shade Response Strategies in Wild Plants: Differential Control of Immunity and Shoot Elongation[OPEN]

Charlotte M.M. Gommers, Diederik H. Keuskamp, Sara Buti, Hans van Veen,[1] Iko T. Koevoets,[2] Emilie Reinen, Laurentius A.C.J. Voesenek, and Ronald Pierik[3]

Plant Ecophysiology, Institute of Environmental Biology, Utrecht University, 3584 CH Utrecht, The Netherlands

ORCID IDs: 0000-0002-0817-5134 (C.M.M.G.); 0000-0002-8973-5518 (I.T.K.); 0000-0002-5320-6817 (R.P.)

Plants growing at high densities elongate their shoots to reach for light, a response known as the shade avoidance syndrome (SAS). Phytochrome-mediated detection of far-red light reflection from neighboring plants activates growth-promoting molecular pathways leading to SAS. However, it is unknown how plants that complete their life cycle in the forest understory and are shade tolerant prevent SAS when exposed to shade. Here, we show how two wild *Geranium* species from different native light environments regulate contrasting responses to light quality cues. A comparative RNA sequencing approach unveiled the molecular underpinnings of their contrasting growth responses to far-red light enrichment. It also identified differential phytochrome control of plant immunity genes and confirmed that far-red enrichment indeed contrastingly affects resistance against *Botrytis cinerea* between the two species. Furthermore, we identify a number of candidate regulators of differential shade avoidance. Three of these, the receptor-like kinases FERONIA and THESEUS1 and the non-DNA binding bHLH protein KIDARI, are functionally validated in *Arabidopsis thaliana* through gene knockout and/or overexpression studies. We propose that these components may be associated with either showing or not showing shade avoidance responses.

INTRODUCTION

Plants have evolved a variety of strategies to deal with environmental stresses. Oftentimes, the underlying regulatory circuits are very well understood in model plants, while alternative strategies in species with a different evolutionary history are not. One example of this is the way in which deetiolated plants adjust to light quality changes.

Plants absorb blue (400–500 nm) and red (600–700 nm) light, but not far-red (700–800 nm) light for photosynthesis. Due to this preferential absorption by leaves the red:far-red light ratio (R:FR) declines in dense vegetation, which is a signal for neighbor proximity. In response, shade intolerant plants prioritize enhanced elongation of their leaf-bearing organs (stems and petioles) over branching, lift their leaves to a more vertical position (hyponasty) to bring their leaves to the top of the canopy, and flower early, a phenomenon known as the shade avoidance syndrome (SAS; reviewed in Pierik and Testerink, 2014; Fraser et al., 2016). Low R:FR-induced shade avoidance is absent in shade-tolerant plants that thrive on the forest floor and cannot outcompete the tall trees surrounding them (Gommers et al., 2013; Valladares and Niinemets, 2008).

Changes in R:FR light are sensed by the phytochrome family of photoreceptors in all higher plants. These photoconvert from the active, FR-absorbing form (Pfr) to the inactive, R-absorbing form (Pr) and vice versa. In direct sunlight (R:FR = 1.1), Pfr localizes to the nucleus, where it binds to a set of basic helix-loop-helix (bHLH) transcription factors, the PHYTOCHROME INTERACTING FACTORs (PIFs). In canopy shade (R:FR < 0.4), PIFs are released when Pfr is photoconverted to Pr and regulate cell elongation by enhancing transcription of growth-promoting genes (Quail, 2002). PIFs directly regulate the expression of genes encoding cell wall modifying proteins, such as *XYLOGLUCAN ENDOTRANSGLUCOSYLASE/HYDROLASE15* (*XTH15*) (Hornitschek et al., 2009). PIFs also directly target genes encoding proteins involved in controlling auxin homeostasis and signaling, which is a major hormone controlling hypocotyl elongation of *Arabidopsis thaliana* seedlings during shade avoidance (Tao et al., 2008; Keuskamp et al., 2010; Li et al., 2012; Hornitschek et al., 2012; Nozue et al., 2015). PIF4 interacts with growth repressing DELLA proteins (Djakovic-Petrovic et al., 2007; de Lucas et al., 2008) and BRASSINAZOLE RESISTANT1 (BZR1; Oh et al., 2012), which are targets of two other growth-regulating hormones, gibberellin and brassinosteroids, respectively.

SAS is a widespread strategy that is accompanied by controlled suppression of jasmonic acid (JA)- and salicylic acid-mediated defenses against pathogens and herbivores (de Wit et al., 2013; Moreno et al., 2009), thus prioritizing consolidation of light capture over other stresses. Arabidopsis plants exposed to low R:FR light are more susceptible to the necrotrophic pathogen *Botrytis cinerea*, as a consequence of stabilization of jasmonate ZIM-domain (JAZ) transcriptional repressors, when

[1] Current address: PlantLab, Institute of Life Sciences, Scuola Superiore Sant'Anna, 56127 Pisa, Italy.
[2] Current address: Plant Cell Biology, Swammerdam Institute for Life Sciences, University of Amsterdam, 1098 XH Amsterdam, The Netherlands.
[3] Address correspondence to r.pierik@uu.nl.
The author responsible for distribution of materials integral to the findings presented in this article in accordance with the policy described in the Instructions for Authors (www.plantcell.org) is: Ronald Pierik (r.pierik@uu.nl).
[OPEN]Articles can be viewed without a subscription.
www.plantcell.org/cgi/doi/10.1105/tpc.16.00790

DELLA proteins are degraded (Chico et al., 2014; Cerrudo et al., 2012; de Wit et al., 2013).

The molecular pathways that stimulate elongation growth would be maladaptive in forest understory plants. Indeed, variation in low R:FR-induced stem elongation rates has been documented between (Morgan and Smith, 1978; Gilbert et al., 2001) and within (Sasidharan et al., 2009; Coluccio et al., 2011; Jiménez-Gómez et al., 2010; Filiault and Maloof, 2012) species. Species from forest understories, in addition to suppressing low R:FR-induced stem elongation, have evolved shade tolerance strategies, such as optimal leaf morphology for low-light photosynthesis (Morgan and Smith, 1978) and tolerance to biotic and abiotic stresses (reviewed in Valladares and Niinemets, 2008). Currently, it remains unknown how shade tolerant species inhibit SAS while being exposed to potent SAS-inducing light signals (Gommers et al., 2013). Identifying the molecular mechanisms underpinning suppression of SAS has great potential to (1) show how different strategies of adaptive plasticity can be regulated and (2) inform crop-breeding programs targeted at minimizing yield losses, which are caused by wasteful carbon investments in nonharvestable stems (Carriedo et al., 2016) and suppressed immunity.

Here, we study responses to changing R:FR light ratios in two *Geranium* species from contrasting habitats: *G. robertianum* (herb Robert), which grows in a wide amplitude of conditions including forest understories, and *G. pyrenaicum* (hedge cranesbill), which occurs in open habitats. In response to low R:FR light conditions, these two species showed highly contrasting growth, transcriptome, and pathogen defense responses. We identified novel putative SAS regulators, which were subsequently confirmed in gene functional studies in Arabidopsis.

RESULTS

G. pyrenaicum and *G. robertianum* Express Opposite Growth Responses to Low R:FR

To study the regulatory pathways that suppress shade avoidance, we exposed two wild *Geranium* species from contrasting habitats to FR-enriched (low R:FR = 0.2) versus control (R:FR = 1.8) white light conditions. *G. pyrenaicum* expressed the classic shade avoidance response by elongating its petioles, whereas this was not apparent in *G. robertianum* (Figures 1A and 1B). Detailed petiole growth kinetics over 24 h (Figure 1C) and 48 h (Supplemental Figure 1A) show that both species initially enhance petiole elongation upon low R:FR treatment. Nevertheless, *G. robertianum* does not show enhanced petiole elongation in low R:FR toward the end of the day and during the night (Figure 1C), regardless of the start time of the treatment (Figure 1D; Supplemental Figure 2). This results in no net difference between the treatments after 24 h in *G. robertianum*. By contrast, *G. pyrenaicum* is always able to rapidly induce petiole elongation upon exposure to low R:FR, independent of the time of day, although

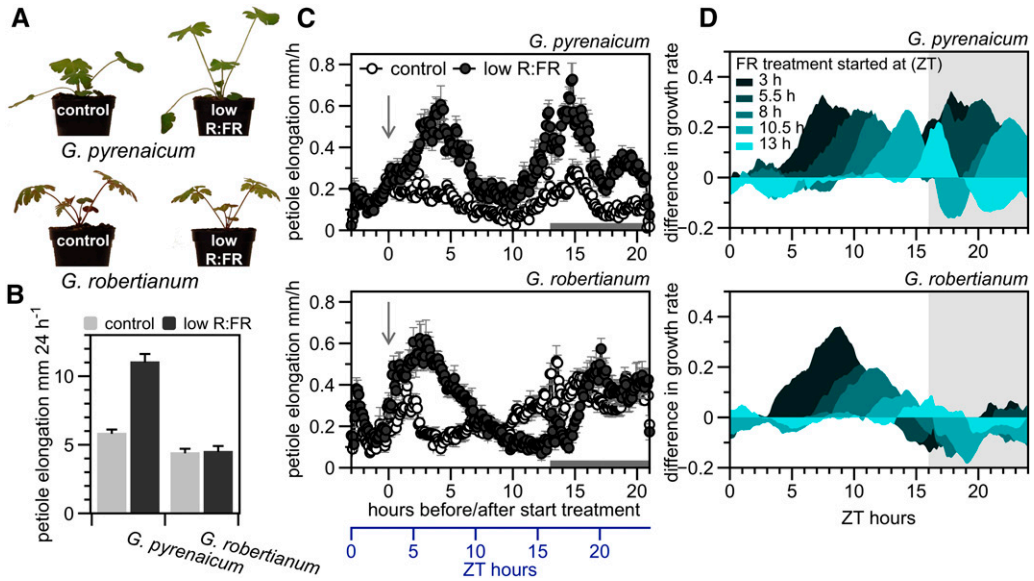

Figure 1. Characterization of *G. pyrenaicum* and *G. robertianum* as Model Species with Opposite Petiole Elongation Responses in Low R:FR Light.

(A) *G. pyrenaicum* and *G. robertianum* plants exposed to control white light (R:FR = 1.8) or a low R:FR (R:FR = 0.2) treatment for 5 d.

(B) Elongation (mm 24 h^{-1}) of the second petiole of *G. pyrenaicum* and *G. robertianum* leaves, exposed to control white light or low R:FR conditions. Data represent means + SE, $n = 7$.

(C) Growth rates of *G. pyrenaicum* and *G. robertianum* petioles in mm h^{-1} over 24 h, data for every 6 min. Plants grown in either control white light (open circles) or a low R:FR treatment (dark circles), starting at time point 0 (ZT = 3 h, indicated by an arrow). Data represent means ± SE, $n = 6$. The gray bar at the *x* axis indicates the night period.

(D) The difference between petiole growth rates (mm h^{-1}) in control and low R:FR treatments with a different starting point during the photoperiod, for a 24-h period (differences for the ZT = 3 h starting point are taken from data presented in **[C]**), in *G. pyrenaicum* (upper graph) and *G. robertianum* (lower graph). Differences between the means of the two treatments are smoothed using exponential smoothing, $n = 6$. The gray area represents the night period.

it suppresses petiole elongation in the night period when treatments started at 17:30 or 20:00 (Figure 1D; Supplemental Figure 2).

In both species, petioles elongated mainly at the apical part, just under the leaf lamina (Supplemental Figures 1B and 1C). Based on these results, we harvested the most responsive apical part of the petiole after 2 and 11.5 h of low R:FR treatment and corresponding controls grown in white light for a transcriptome analysis to investigate the gene expression profiles associated with these growth differences.

De Novo Assembly of *Geranium* Transcriptomes and Comparison to Plant Model Species

Two *Geranium* reference transcriptomes were assembled de novo from combined Illumina-sequenced normalized and non-normalized libraries to establish maximum transcript coverage. Using the Markov Clustering Algorithm (OMCL; Enright et al., 2002) with an inflation factor (I) of 3.0, transcripts were clustered into putatively orthologous transcript groups. All low-abundant OMCL groups (<20 reads) were removed without affecting the number of differentially expressed OMCL groups during further analysis (Figures 2A and 2B). Of the 26,434 OMCL groups, 51% was shared by the two species (Figure 2B), and lowering the I increased this to 74%, at the cost of solely *G. robertianum* OMCL groups (~28% with I = 3.0 to ~5% with I = 1.1; Figure 2B), indicating that this species has many transcript variants, while being considered a diploid, as is *G. pyrenaicum* (Warburg, 1938; Tofts, 2004). Accordingly, most OMCL groups contained only one *G. pyrenaicum*, but more than one *G. robertianum* transcript (Figure 2D; I = 3.0 and <20 reads).

Geranium transcriptomes were compared with model species Arabidopsis, tomato (*Solanum lycopersicum*), beet (*Beta vulgaris*) and rice (*Oryza sativa*), using OMCL clustering with I = 1.1 (and >20 reads for *Geranium* transcripts). As shown in Figure 2C, 2251 OMCL groups were shared among all six species, 1480 covered only *Geranium* transcripts, and only two OMCL groups were present in all species but not identified in *Geranium*. Our two species showed strong overlap with beet (~88%), tomato (~82%), and Arabidopsis (~77%).

Transcriptome Analysis of *G. pyrenaicum* and *G. robertianum* Exposed to Low R:FR Light

To identify transcriptional changes upon 2 or 11.5 h of low R:FR in the two species, we mapped Illumina sequenced reads of the non-normalized libraries (constructed from the apical half of petioles in control or low R:FR light at the two time points) to the newly

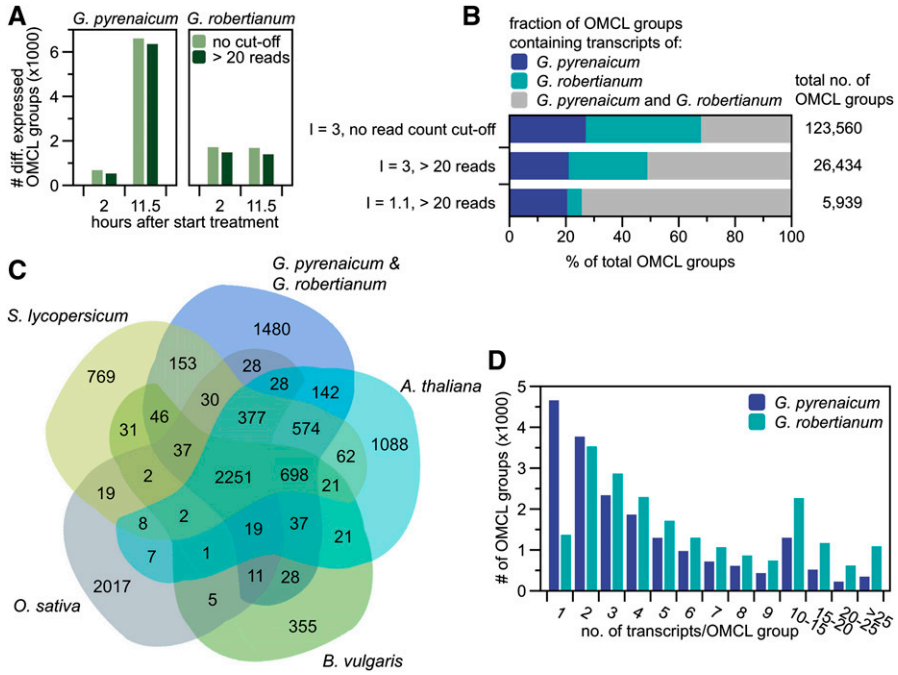

Figure 2. *Geranium* Transcriptome Assembly and Clustering of Putatively Orthologous Transcripts.

(A) Effect of the read count cutoff of 20 on the number of differentially expressed OMCL groups (I = 3.0 and > 20 reads, low R:FR versus control, $P < 0.01$) for both species at the two time points.

(B) Fractions (in %) of ortho Markov-clustered groups containing transcripts of *G. pyrenaicum*, *G. robertianum*, or both, with two different inflation factors (3.0 versus 1.1) and with or without an applied read count cutoff of 20 for at least one of the treatments/time points. The total number of OMCL groups for the three different settings is given at the right side of the graph.

(C) Ortholog transcript distribution over six species (*G. pyrenaicum*, *G. robertianum*, Arabidopsis, *B. vulgaris*, *O. sativa*, and *S. lycopersicum*) in a plant kingdom-wide clustering, using OMCL (I = 1.1, *Geranium* read counts > 20). *G. pyrenaicum* and *G. robertianum* OMCL groups are pooled for the figure.

(D) OMCL group sizes (no. of transcripts) for both species separate (I = 3.0 and > 20 counts).

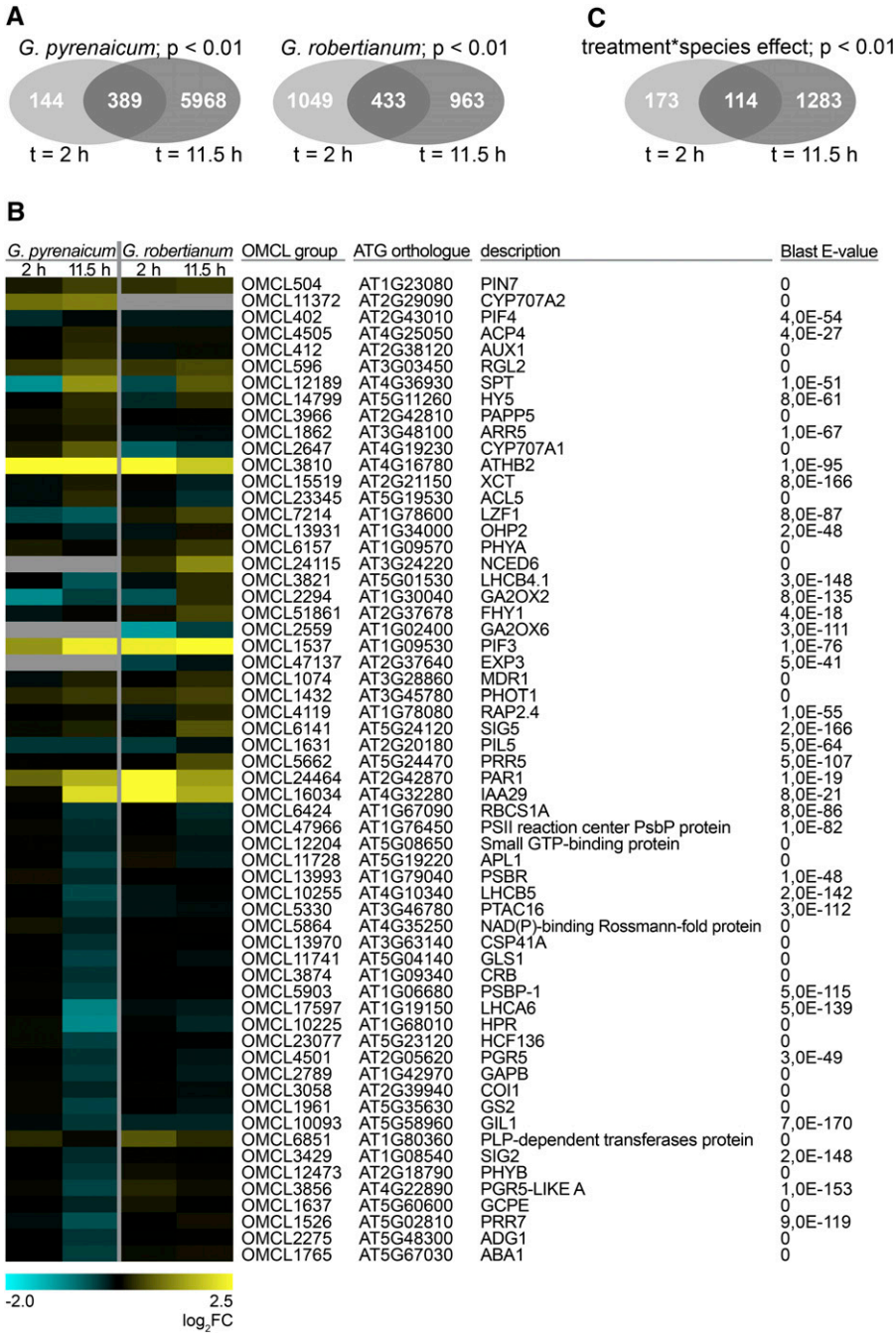

OMCL group	ATG orthologue	description	Blast E-value
OMCL504	AT1G23080	PIN7	0
OMCL11372	AT2G29090	CYP707A2	0
OMCL402	AT2G43010	PIF4	4,0E-54
OMCL4505	AT4G25050	ACP4	4,0E-27
OMCL412	AT2G38120	AUX1	0
OMCL596	AT3G03450	RGL2	0
OMCL12189	AT4G36930	SPT	1,0E-51
OMCL14799	AT5G11260	HY5	8,0E-61
OMCL3966	AT2G42810	PAPP5	0
OMCL1862	AT3G48100	ARR5	1,0E-67
OMCL2647	AT4G19230	CYP707A1	0
OMCL3810	AT4G16780	ATHB2	1,0E-95
OMCL15519	AT2G21150	XCT	8,0E-166
OMCL23345	AT5G19530	ACL5	0
OMCL7214	AT1G78600	LZF1	8,0E-87
OMCL13931	AT1G34000	OHP2	2,0E-48
OMCL6157	AT1G09570	PHYA	0
OMCL24115	AT3G24220	NCED6	0
OMCL3821	AT5G01530	LHCB4.1	3,0E-148
OMCL2294	AT1G30040	GA2OX2	8,0E-135
OMCL51861	AT2G37678	FHY1	4,0E-18
OMCL2559	AT1G02400	GA2OX6	3,0E-111
OMCL1537	AT1G09530	PIF3	1,0E-76
OMCL47137	AT2G37640	EXP3	5,0E-41
OMCL1074	AT3G28860	MDR1	0
OMCL1432	AT3G45780	PHOT1	0
OMCL4119	AT1G78080	RAP2.4	1,0E-55
OMCL6141	AT5G24120	SIG5	2,0E-166
OMCL1631	AT2G20180	PIL5	5,0E-64
OMCL5662	AT5G24470	PRR5	5,0E-107
OMCL24464	AT2G42870	PAR1	1,0E-19
OMCL16034	AT4G32280	IAA29	8,0E-21
OMCL6424	AT1G67090	RBCS1A	8,0E-86
OMCL47966	AT1G76450	PSII reaction center PsbP protein	1,0E-82
OMCL12204	AT5G08650	Small GTP-binding protein	0
OMCL11728	AT5G19220	APL1	0
OMCL13993	AT1G79040	PSBR	1,0E-48
OMCL10255	AT4G10340	LHCB5	2,0E-142
OMCL5330	AT3G46780	PTAC16	3,0E-112
OMCL5864	AT4G35250	NAD(P)-binding Rossmann-fold protein	0
OMCL13970	AT3G63140	CSP41A	0
OMCL11741	AT5G04140	GLS1	0
OMCL3874	AT1G09340	CRB	0
OMCL5903	AT1G06680	PSBP-1	5,0E-115
OMCL17597	AT1G19150	LHCA6	5,0E-139
OMCL10225	AT1G68010	HPR	0
OMCL23077	AT5G23120	HCF136	0
OMCL4501	AT2G05620	PGR5	3,0E-49
OMCL2789	AT1G42970	GAPB	0
OMCL3058	AT2G39940	COI1	0
OMCL1961	AT5G35630	GS2	0
OMCL10093	AT5G58960	GIL1	7,0E-170
OMCL6851	AT1G80360	PLP-dependent transferases protein	0
OMCL3429	AT1G08540	SIG2	2,0E-148
OMCL12473	AT2G18790	PHYB	0
OMCL3856	AT4G22890	PGR5-LIKE A	1,0E-153
OMCL1637	AT5G60600	GCPE	0
OMCL1526	AT5G02810	PRR7	9,0E-119
OMCL2275	AT5G48300	ADG1	0
OMCL1765	AT5G67030	ABA1	0

Figure 3. Low R:FR Light Differentially Affects *G. pyrenaicum* and *G. robertianum* Gene Expression.

(A) Venn diagrams representing overlap of the differentially expressed OMCL groups upon the low R:FR treatment (up- and downregulated, $P < 0.01$, qCML method, followed by an exact test) between the two different time points for *G. pyrenaicum* (upper) and *G. robertianum* (lower) separately.

(B) Heat map representing expression values of *Geranium* orthologs of Arabidopsis genes appointed to the GO terms "R or FR light signaling pathway," "response to R or FR light," "shade avoidance," "response to R light," "response to FR light," "R light signaling pathway," and/or "FR light signaling pathway," which are significantly ($P < 0.01$, qCML method, followed by an exact test) induced or repressed by a low R:FR treatment at at least one time point (2 or 11.5 h) in at least one species (*G. pyrenaicum* or *G. robertianum*). Colors represent the $\log_2$ fold change upon the low R:FR treatment. The ATG code and description of the closest Arabidopsis ortholog is given for each *Geranium* OMCL group, with matching E-value of the BLAST hit. Gray areas represent the absence of this OMCL group in this species.

(C) Venn diagram showing the number of OMCL groups with a significant treatment*species interaction ($P < 0.01$, glmLRT) and overlap between the two time points.

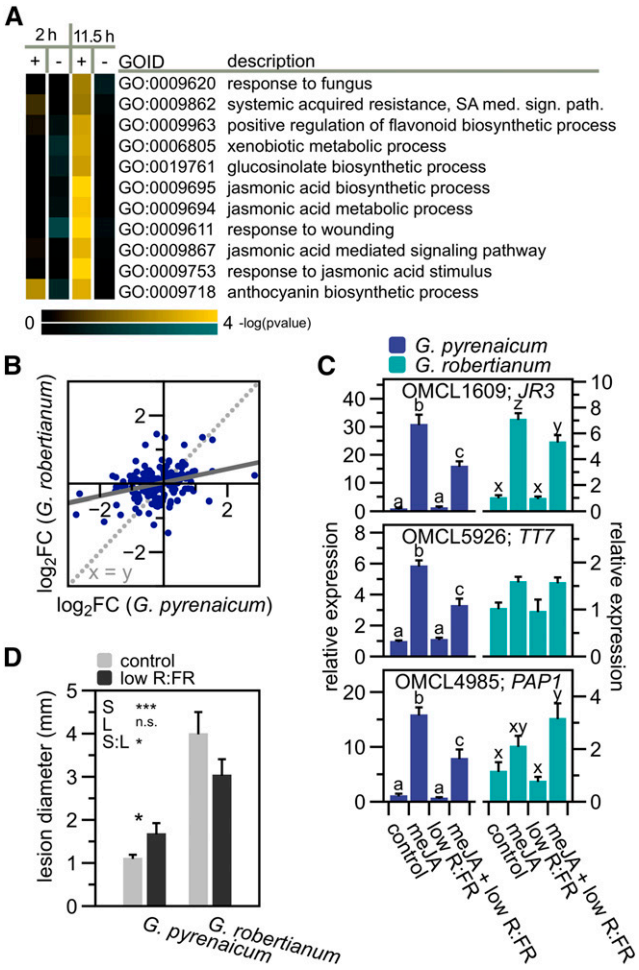

Figure 4. Low R:FR Light Differentially Affects *G. pyrenaicum* and *G. robertianum* Immunity.

(A) Heat map of the gene ontology clusters overrepresenting transcripts with a positive species*treatment interaction (log_2 fold changes are significantly higher in *G. robertianum* compared with *G. pyrenaicum*) at t = 11.5 h, and a role in plant defenses against pests. Colors represent the -log of the adjusted P value, where blue is a negative interaction (*G. pyrenaicum* fold change > *G. robertianum* fold change) and yellow is a positive interaction (*G. pyrenaicum* < *G. robertianum*).

(B) Scatterplot of the log fold changes (low R:FR versus control) in *G. pyrenaicum* (*x* axis) and *G. robertianum* (*y* axis) of transcripts attributed to the gene ontology clusters presented in **(A)**.

(C) Expression data of the *Geranium* orthologs of *JR3*, *TT7*, and *PAP1* upon 100 μM methyl-JA, low R:FR (R:FR = 0.2, 2 h), or combined treatment, relative to the control (R:FR = 1.8, mock) and the reference gene (ortholog of *PDF1*), in *G. pyrenaicum* (light blue) and *G. robertianum* (dark blue) leaves (petiole + lamina). Chemicals (250 μL) were sprayed on the leaf at the start of the light treatment. Data represent means + SE, $n = 5$ (biological replicates are a pool of the second leaf of two individual plants) Different letters represent significant differences (two-way ANOVA and post-hoc Tukey test, $P < 0.05$).

(D) Lesion diameters (mm) of a *B. cinerea* infection (2 μL of 2.5×10^5 spores mL^{-1}) on *G. pyrenaicum* and *G. robertianum* cotyledons, in a control or low R:FR light environment, measured 3 d after inoculation. Data represent means ±SE, $n = 28$. Asterisks represent significant differences (two-way ANOVA and post-hoc Tukey test, $P < 0.05$).

constructed transcriptomes. Read counts of all contigs in an OMCL group were summed before further statistical analysis.

In *G. pyrenaicum*, 533 OMCL groups were differentially regulated after 2 h of low R:FR light, and this increased after 11.5 h to 6.357 (Figure 3A). In *G. robertianum*, the numbers of differentially expressed OMCL groups were comparable at the two time points (1.482 at t = 2 h; 1.396 at t = 11.5 h; Figure 3A). Matching the contrasting petiole elongation phenotypes of these species in low R:FR light, expression of *Geranium* orthologs of several SAS-associated genes (binned to the Gene Ontology [GO] terms "R or FR light signaling pathway," "response to R or FR light," "shade avoidance," "response to R light," "response to FR light," "R light signaling pathway," and/or "FR light signaling pathway" in Arabidopsis) was different between the two species, especially at time point t = 11.5 h (Figure 3B). GO clustering of all up- and downregulated OMCL groups (Supplemental Figure 3) shows that both species upregulate "shade avoidance"-related, as well as several hormone- and cell wall-related genes. Photosynthesis-associated ontologies were enriched among downregulated OMCL groups, which would be in accordance with previous studies that show how phytochrome inactivation can repress photosynthetic capacity (Toledo-Ortiz et al., 2010; Yang et al., 2016).

As shown by the large number of OMCL groups with a significant treatment*species interaction, most differences in low R:FR-induced expression between the species occurred in the later time point (1.397 OMCL groups, compared with 287 at t = 2 h; Figure 3C), matching the growth patterns shown in Figure 1.

A GO analysis on the OMCL groups with a significant treatment*species interaction (Supplemental Figure 4) revealed that after 2 h of low R:FR, the OMCL groups with a species*treatment interaction larger than zero (which represents significantly higher log_2 fold changes for *G. robertianum* than *G. pyrenaicum*) were overrepresented in the GO category for shade avoidance. At the second time point, the OMCL groups with a negative interaction were overrepresented in SAS-related GO categories, such as brassinosteroid metabolic process, cell wall compounds, and response to light stimulus.

JA-Mediated Defenses Are Repressed by Low R:FR in *G. pyrenaicum* but Enhanced in *G. robertianum*

Among the GO categories with a strong positive interaction effect in the evening, we identified several defense-associated ontologies (Supplemental Figure 4; Figure 4A). Many OMCL groups with possible functions in the JA-mediated defense against herbivores or necrotrophic pathogens appeared to be downregulated after 11.5 h of low R:FR treatment in *G. pyrenaicum*, but not, or to a lesser extent, in *G. robertianum* (Figure 4B; Supplemental Figure 5A). Downregulation of defense pathways by low R:FR has also been described in Arabidopsis (Cargnel et al., 2014; Cerrudo et al., 2012; de Wit et al., 2013) and tomato (Cortés et al., 2016). *Geranium* orthologs of JA-inducible genes *JASMONIC ACID RESPONSIVE3* (*JR3*), *TRANSPARENT TESTA7* (*TT7*), and *PRODUCTION OF ANTHOCYANIN PIGMENT1* (*PAP1*) were transcriptionally induced by a methyl-JA treatment, but this induction was suppressed by simultaneous exposure to low R:FR light in *G. pyrenaicum* (Figure 4C), similar to what was previously shown in Arabidopsis (de Wit et al., 2013; Supplemental

Figure 5B). Interestingly, *G. robertianum* lacks the reduction in defenses observed in *G. pyrenaicum*. These data hint at differential control of immunity by R:FR between the two species. To examine the biological consequences of these differences, cotyledons of both species were infected with spores of the necrotrophic pathogen *B. cinerea* under control and low R:FR light. Consistent with the gene expression patterns, lesion diameters caused by the pathogen increased in the low R:FR treatment in *G. pyrenaicum*, but decreased in *G. robertianum* (Figure 4D). These data indicate that the divergence of R:FR responses between these species extends to pathogen resistance. *G. robertianum* shows higher background susceptibility to *B. cinerea* than *G. pyrenaicum*, and this may be associated with differences in leaf structure between the two species. Low R:FR-mediated petiole elongation in the seedlings (cotyledon petioles), however, remained unaffected by the *B. cinerea* treatment and was pronounced in *G. pyrenaicum* and absent in *G. robertianum* (Supplemental Figure 5C).

Candidate OMCL Group Selection for Differential Low R:FR-Induced Growth Patterns

To find OMCL groups that might be functionally associated with the low R:FR-induced growth patterns of the *Geranium* species, we selected the groups upregulated in both time points in *G. pyrenaicum*, but only in the early time point in *G. robertianum* (Figure 5A). Among this selection of 31 OMCL groups (Figure 5B) were orthologs of some known downstream SAS components, such as *GIBBERELLIC ACID 20 OXIDASE2* (*GA20OX2*), *XYLOGLUCAN ENDOTRANSGLUCOSYLASE/HYDROLASE9*

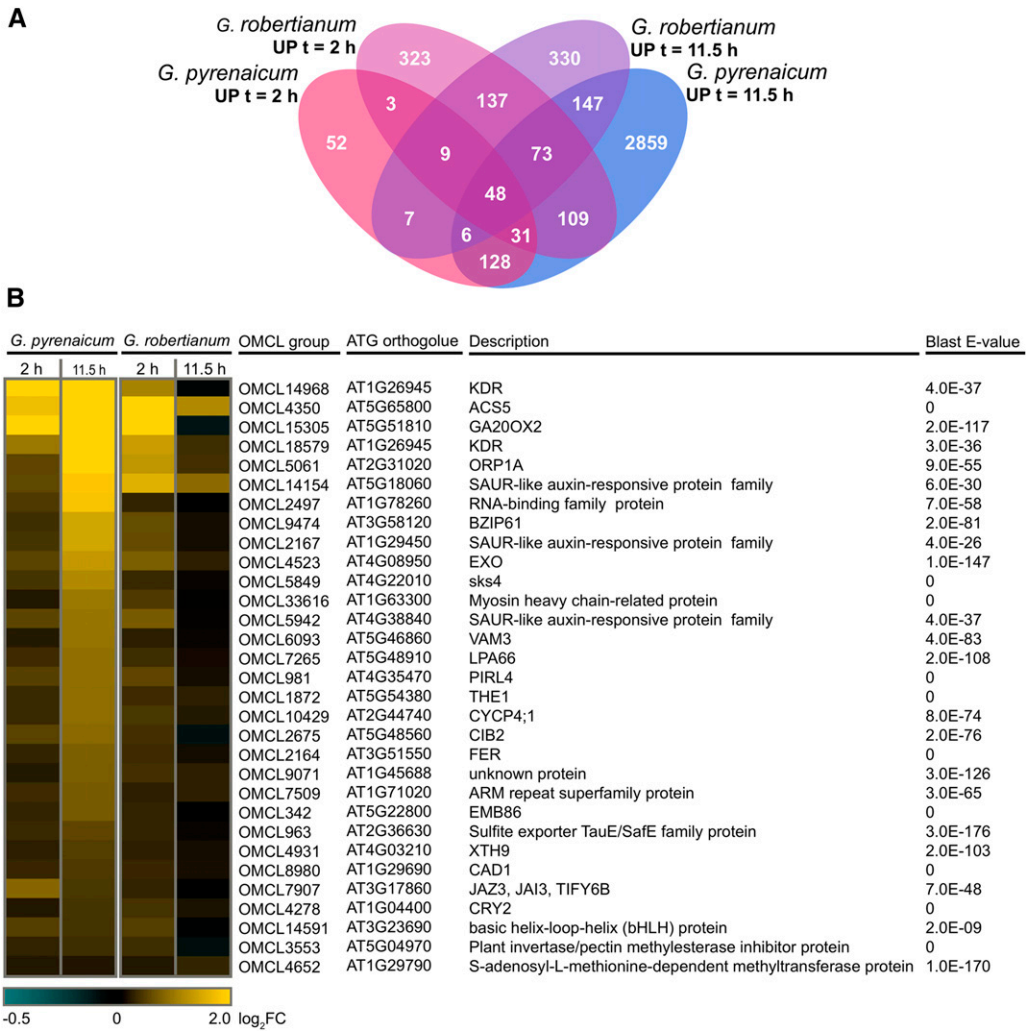

OMCL group	ATG orthogolue	Description	Blast E-value
OMCL14968	AT1G26945	KDR	4.0E-37
OMCL4350	AT5G65800	ACS5	0
OMCL15305	AT5G51810	GA20OX2	2.0E-117
OMCL18579	AT1G26945	KDR	3.0E-36
OMCL5061	AT2G31020	ORP1A	9.0E-55
OMCL14154	AT5G18060	SAUR-like auxin-responsive protein family	6.0E-30
OMCL2497	AT1G78260	RNA-binding family protein	7.0E-58
OMCL9474	AT3G58120	BZIP61	2.0E-81
OMCL2167	AT1G29450	SAUR-like auxin-responsive protein family	4.0E-26
OMCL4523	AT4G08950	EXO	1.0E-147
OMCL5849	AT4G22010	sks4	0
OMCL33616	AT1G63300	Myosin heavy chain-related protein	0
OMCL5942	AT4G38840	SAUR-like auxin-responsive protein family	4.0E-37
OMCL6093	AT5G46860	VAM3	4.0E-83
OMCL7265	AT5G48910	LPA66	2.0E-108
OMCL981	AT4G35470	PIRL4	0
OMCL1872	AT5G54380	THE1	0
OMCL10429	AT2G44740	CYCP4;1	8.0E-74
OMCL2675	AT5G48560	CIB2	2.0E-76
OMCL2164	AT3G51550	FER	0
OMCL9071	AT1G45688	unknown protein	3.0E-126
OMCL7509	AT1G71020	ARM repeat superfamily protein	3.0E-65
OMCL342	AT5G22800	EMB86	0
OMCL963	AT2G36630	Sulfite exporter TauE/SafE family protein	3.0E-176
OMCL4931	AT4G03210	XTH9	2.0E-103
OMCL8980	AT1G29690	CAD1	0
OMCL7907	AT3G17860	JAZ3, JAI3, TIFY6B	7.0E-48
OMCL4278	AT1G04400	CRY2	0
OMCL14591	AT3G23690	basic helix-loop-helix (bHLH) protein	2.0E-09
OMCL3553	AT5G04970	Plant invertase/pectin methylesterase inhibitor protein	0
OMCL4652	AT1G29790	S-adenosyl-L-methionine-dependent methyltransferase protein	1.0E-170

Figure 5. Selection of Candidate Genes from the Transcriptome Analysis to Explain Low R:FR-Induced Growth Patterns in Geraniums.

(A) Venn diagram presenting OMCL groups significantly upregulated in low R:FR (R:FR = 0.2) versus control (R:FR = 1.8) (adjusted $P < 0.01$, read counts > 20) in both species after 2 (red shades) or 11.5 h (blue shades).

(B) The selection of 31 OMCL groups, upregulated in *G. pyrenaicum* after 2 and 11.5 h, and in *G. robertianum* after 2 h (from 5A), with the closest Arabidopsis ortholog, description, and BLAST E-value. Colors represent the $\log_2$ fold change.

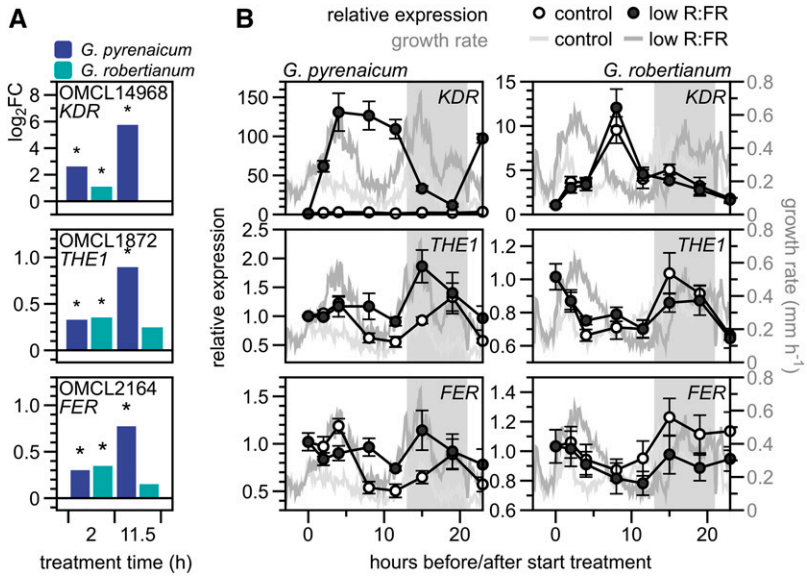

Figure 6. *G. pyrenaicum* and *G. robertianum* Differentially Express *KDR*, *THE1*, and *FER* in Low R:FR Light over Time.

(A) Log_2 fold changes of OMCL14968 (*KDR* ortholog), OMCL1872 (*THE1*), and OMCL2164 (*FER*) in *G. pyrenaicum* (dark-blue bars) and *G. robertianum* (turquoise bars). Asterisks represent significant transcriptional regulation (low R:FR versus control, adjusted $P < 0.01$, qCML method, followed by an exact test). **(B)** Relative OMCL group expression over time in *G. pyrenaicum* (left panels) and *G. robertianum* (right panels) petioles in control (open circles) and low R:FR (dark circles) on the left *y* axis. Data are relative to the reference gene (ortholog of *PDF1*) and to t = 0 (10:00 am) and represent means ± SE, $n = 5$ (biological replicates are a pool of the second petiole of three individual plants). Right *y* axis and gray lines represent growth rates in mm h^{-1} over the same time period in control (light gray) and low R:FR (darker gray) conditions (same data as Figure 1C). Gray area represents the night period.

(*XTH9*), and several *SMALL AUXIN REGULATED RNAs* (*SAURs*). In a search for potential upstream differential components, we selected bHLH transcription factor *KIDARI* (*KDR*) and two members of the family of *Catharanthus roseus* receptor-like kinases (CrRLKs): *THESEUS1* (*THE1*) and *FERONIA* (*FER*) (Figure 6A). Transcription of these OMCL groups was analyzed using RT-qPCR in more detailed kinetics and plotted together with petiole elongation rates (Figure 6B). *KDR* expression was rapidly and strongly upregulated by low R:FR in *G. pyrenaicum* and dropped during the night. Low R:FR-induced transcription of

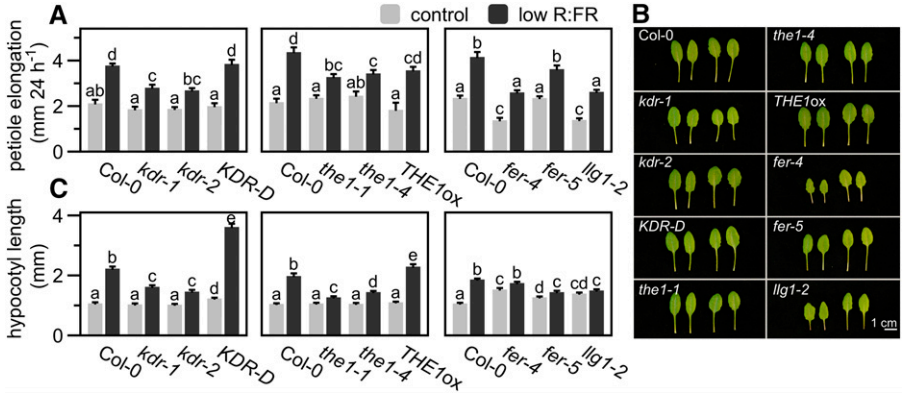

Figure 7. Functional Analysis of *KDR*, *THE1*, *FER*, and *LLG1* in Low R:FR-Exposed Arabidopsis Rosettes and Seedlings Reveals Functions in Regulating Elongation of Petioles and Hypocotyls.

(A) and **(B)** Petiole elongation (mm) of several *KDR*, *THE1*, *FER*, and *LLG1* deficient and overexpressing lines compared with the wild-type control (Col-0), grown in control white light (R:FR = 1.8, light gray bars) or low R:FR (R:FR = 0.2, dark gray bars) conditions for 24 h (data represent means + SE, $n = 10$. Different letters indicate significant differences; $P < 0.05$, two-way ANOVA with post-hoc Tukey test) **(A)**, with representative photographs of leaves grown in control (left pairs) or low R:FR (right pairs) for 5 d **(B)**.

(C) Hypocotyl length (mm) of Arabidopsis lines shown in **(A)** after 4 d of control white light or low R:FR treatment. Data represent means + SE, $n = 40$. Different letters indicate significant differences ($P < 0.05$, two-way ANOVA with post-hoc Tukey test).

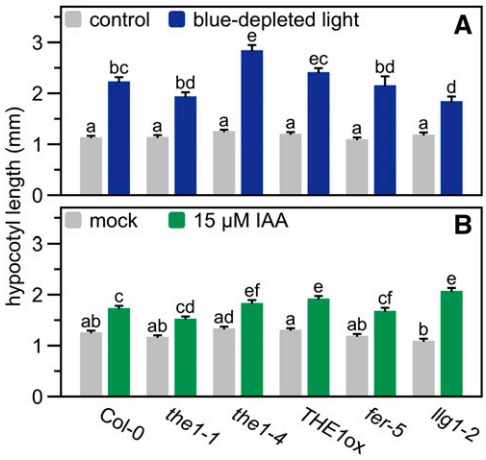

Figure 8. RLKs Have No Function in Blue Light-Depleted- and Auxin-Mediated Hypocotyl Elongation.

Hypocotyl length (mm) of Arabidopsis *THE1*-, *FER*-, and *LLG1*-deficient and -overexpressing lines and the wild-type control (Col-0) after 4 d of control white light (±60 μmol m^{-2} s^{-1} blue) and blue light depleted (±4 μmol m^{-2} s^{-1} blue light) **(A)**, or mock (0.1% DMSO) and 15 μM IAA treatment (in 0.1% DMSO) **(B)**. Data represent means + SE, $n = 40$. Different letters indicate significant differences ($P < 0.05$, two-way ANOVA with post-hoc Tukey test).

THE1 and *FER* was slower and weaker than *KDR*, peaking at the beginning of the night. All three OMCL groups are hardly up-regulated in the low R:FR-treated *G. robertianum* petioles, and expression is even slightly inhibited in the night. Expression of a number of other OMCL groups from the cluster of 31, including *GA20OX2* and transcription factors *BZIP61* and *CIB2*, was also confirmed with RT-qPCR to match the RNA seq patterns (Supplemental Figures 6A and 6B).

Heterologous Studies in Arabidopsis Confirm a Role for *KDR*, *THE1*, and *FER* in SAS

To functionally test the importance of *KDR*, *THE1*, and *FER* in the regulation of SAS, we continued in the model species Arabidopsis because transgenic methods are currently unavailable in *Geranium* species. Petioles of a *KDR* knockout (*kdr-1*; Supplemental Figure 7A) and knockdown (*kdr-2*; Supplemental Figure 7A) line had reduced responses to low R:FR treatment, whereas the activation tagged line *KDR-D* (Supplemental Figure 7B) was similar to Col-0 wild type (Figures 7A and 7B). In young seedlings, these differences were more extreme. Hypocotyls of *kdr-1* and *kdr-2* were strongly inhibited in low R:FR-induced elongation and *KDR-D* was hypersensitive to low R:FR (Figure 7C).

The *THE1* knockout *the1-4*, loss-of-function missense mutant *the1-1*, and the *HERKULES1* (*HERK1*; a related RLK that was previously shown to act redundantly to *THE1* in regulating hypocotyl, petiole and lamina cell growth; Guo et al., 2009) *THE1* double mutant *herk1 the1* showed significantly reduced low R:FR-induced petiole elongation (Figures 7A and 7B; Supplemental Figures 8A and 8B). On the other hand, *THE1*ox responded similarly to the wild type (Figures 7A and 7B). Hypocotyls of *the1-1*, *the1-4*, and *herk1 the1* seedlings showed severe low R:FR-induced elongation defects, whereas *THE1*ox showed an exaggerated response compared with Col-0 (Figure 7C; Supplemental Figure 8C). Consistent with the known *THE1-HERK1* redundancy, the *herk1* single mutant responded similar to Col-0 (Supplemental Figures 8A to 8C).

Adult *FER* knockdown (*fer-5*) and knockout (*fer-4*) plants, as well as the mutant of the FER coreceptor LORELEI-LIKE GPI-AP1 (LLG1; Li et al., 2015) *llg1-2*, all displayed petiole elongation responses to low R:FR that were similar to the wild type (Figures 7A and 7B). However, these mutations dramatically reduced low R:FR-induced hypocotyl elongation: *fer-4*, *fer-5*, and *llg1-2* seedlings lacked this response completely (Figure 7C). Interestingly, although all our candidate genes were found in petiole tissue in rosette-stage *Geranium*, their functional role is particularly striking in Arabidopsis seedlings.

We exposed *the1-1*, *the1-4*, *THE1*ox, *fer-5*, and *llg1-2* seedlings to blue-depleted light (Figure 8A), another shade cue that induces strong elongation (Keuskamp et al., 2011), or 15 μM indole-3-acetic acid (IAA, auxin; Figure 8B). Even though variation in the responses existed, all genotypes would still strongly elongate hypocotyls in these treatments with some variation between different mutants for the same gene, but without a consistent reduction as seen in the low R:FR treatment. This indicates that these RLKs are particularly important for low R:FR-induced hypocotyl elongation, rather than being generic hypocotyl elongation regulators.

Finally, we established whether these novel SAS regulators are transcriptionally regulated in response to low R:FR in Arabidopsis as observed in *G. pyrenaicum*. We analyzed the expression of the *KDR*, *THE1*, *FER*, and SAS marker genes *IAA19* and *ATHB2* in petioles of wild-type Arabidopsis, as well as *pif7*, *pif4 pif5*, and *pif4 pif5 pif7* mutants, using RT-qPCR. *KDR* expression was induced in petioles and was abolished solely in the *pif4 pif5 pif7* triple mutant, while *IAA19* and *ATHB2* expression in low R:FR was partly, but not completely, dependent on PIF4, PIF5, and PIF7 (Figure 9A). *THE1* transcription increased only marginally in low R:FR light in Col-0 and *pif7*, while *FER*, *HERK1*, and *HERK2* expression remained completely unchanged by the light treatment (Figure 9A; Supplemental Figure 8D) in Arabidopsis.

Since *kdr*, *the1*, and *fer* mutations resulted in clear hypocotyl elongation defects in low R:FR-exposed seedlings, we next analyzed the expression of these candidate genes, as well as of *IAA19* and *ATHB2* in hypocotyls of the wild type, *pif7* (with severely suppressed SAS in seedlings; Li et al., 2012), *kdr-1*, *the1-1*, and *fer-5* (Figure 9B). *KDR* and *THE1* expression were, similar to *IAA19*, induced by low R:FR in all genotypes but *pif7*, which lacked this response completely. *FER* expression remained unchanged in all genotypes but was slightly repressed in low R:FR-exposed *pif7* seedlings. Surprisingly, *ATHB2* induction by low R:FR light was absent in *pif7*, *kdr-1*, and *fer-5*, but not in *the1-1*.

Consistent with these expression data, results summarized from previously published transcriptome studies also indicated that low R:FR light, auxin treatments, and *pif* mutations have marginal effects on expression of *FER*, *THE1*, and related RLKs (Supplemental Figure 9). These relatively weak inductions found in

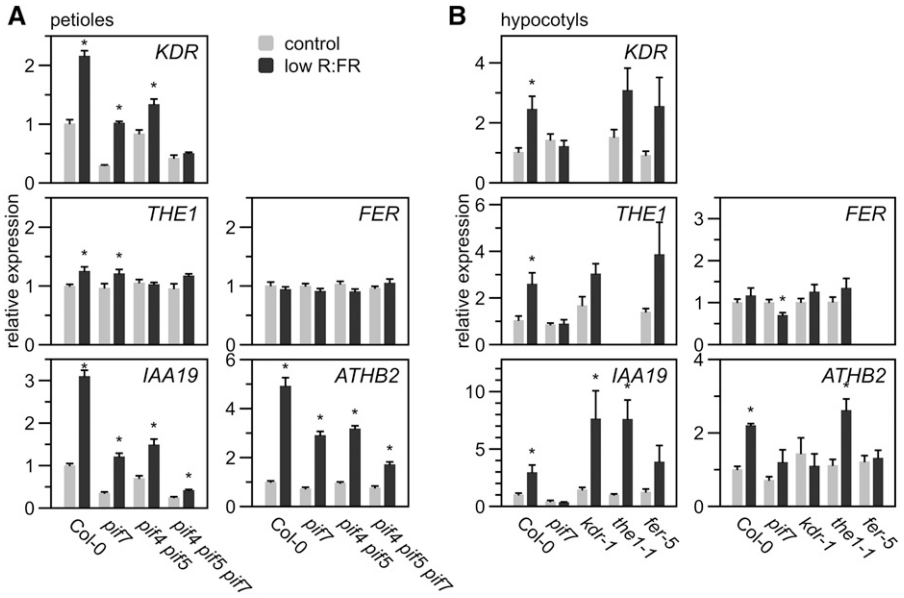

Figure 9. Transcriptional Regulation of *KDR*, *THE1*, and *FER* in Low R:FR Light-Exposed Arabidopsis.

Relative expression of *KDR*, *THE1*, *FER*, *IAA19*, and *ATHB2* in petioles of Col-0, *pif7*, *pif4 pif5*, or *pif4 pif5 pif7* exposed to control white (R:FR = 1.8) or low R:FR light (R:FR = 0.2) for 4 h (values are relative to reference genes and Col-0 in control treatment, data represent means + SE, $n = 6$ biological replicates) **(A)** and in hypocotyls of Col-0, *pif7*, *kdr-1*, *the1-1*, and *fer-5* exposed to the same treatments for 24 h (values are relative to reference genes and Col-0 in control conditions; data represent means + SE, $n = 4$ biological replicates) **(B)**. Asterisks indicate significant differences between the treatments (Student's *t* test, $P < 0.05$).

published data sets may be related to their use of whole shoots or seedlings: Two recent studies on organ-specific gene expression also find more clear induction of *THE1* and *FER* expression in Arabidopsis hypocotyls (Das et al., 2016; Kohnen et al., 2016).

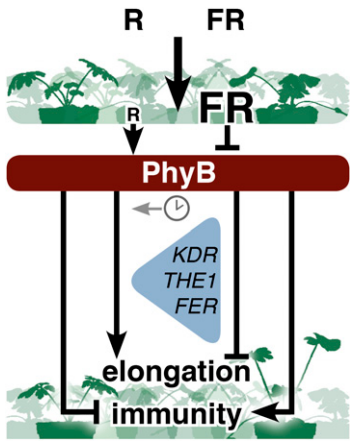

Figure 10. Schematic Overview of How R:FR Light in Plant Canopies Differentially Affects Elongation and Immunity in *G. robertianum* (Left) and *G. pyrenaicum* (Right) upon Phytochrome Deactivation.

KDR, THE1, and FER act downstream of PhyB to regulate elongation and are differentially regulated between the two species. In *G. robertianum*, petiole growth and the transcriptional induction of these genes are suppressed at a specific time of the day (indicated with the clock symbol). In Arabidopsis, these three proteins are positive regulators of low R:FR-induced growth, and *KDR* and *THE1* are transcriptionally induced in a PIF-dependent manner.

DISCUSSION

Our transcriptomics approach in wild species with opposite ecologies and consequently contrasting light quality responses has identified molecular patterns associated with contrasting ecological strategies and novel regulators of shade avoidance responses. *G. pyrenaicum* and *G. robertianum* appear to be a promising comparative model system to study SAS and its suppression, both at a growth-physiological and a transcriptomic level.

The two species respond differently to low R:FR not only at the level of plant architecture, but also in immunity (summarized in Figure 10). It has been shown in Arabidopsis, and other shade avoiding species, that low R:FR light conditions reduce defense responses against herbivorous insects and both necrotrophic and biotrophic pathogens that involve JA- or salicylic acid-mediated signaling (de Wit et al., 2013; Cargnel et al., 2014; Cerrudo et al., 2012; Moreno et al., 2009; Izaguirre et al., 2006). We show here that *G. robertianum*, which occurs in forest understories, enhances its immunity against the fungal pathogen *B. cinerea* upon shade detection, rather than the reduced immunity observed in shade avoiding Arabidopsis and *G. pyrenaicum*. The mechanism through which low R:FR reduces pathogen resistance in shade-intolerant plants is not yet fully established but involves upregulation of the JAZ proteins, which are negative regulators of the JA pathway (Moreno et al., 2009; Cerrudo et al., 2012; Campos et al., 2016). Indeed, the *Geranium* ortholog of *JAZ3* (OMCL7907) is induced by low R:FR in the evening in *G. pyrenaicum*, but not in *G. robertianum* (Figure 5B). We speculate that differential *JAZ* transcript accumulation between the two *Geranium*

species in response to phytochrome inactivation under low R:FR could lead to the observed differential control of immunity.

From the *Geranium* transcriptome, we identified *KDR*, *FER*, and *THE1* as novel candidate genes regulating shade avoidance in response to low R:FR and their involvement was confirmed in heterologous gene functional studies in Arabidopsis (Figure 7). The atypical non-DNA binding bHLH transcription factor KDR has previously been shown to bind, and functionally inhibit, another atypical bHLH protein, LONG HYPOCOTYL IN FAR-RED LIGHT1 (HFR1) (Hyun and Lee, 2006; Hong et al., 2013), a well-studied suppressor of PIF4 and PIF5 function (Hornitschek et al., 2009). Furthermore, *KDR* transcription is directly regulated by the PIF4-BZR1 complex (Oh et al., 2012; Bai et al., 2012). Our expression data in Arabidopsis *pif* mutants showed that *KDR* expression in petioles depends on functional PIF4, PIF5, and PIF7 in both white light and low R:FR (Figure 9A), while in hypocotyls of young seedlings it solely depends on PIF7. Nevertheless, *KDR* had not previously been identified as a low R:FR-inducible functional regulator of SAS. The strong differences in expression levels between the *Geranium* species and its presumed interaction with a modulator of PIF activity, HFR1, make KDR an interesting candidate regulating the two different strategies in the shade. However, since we could not identify *HFR1* orthologs in the *Geranium* transcriptomes, it is possible that KDR in these species interacts with other regulators, potentially other bHLH proteins, to suppress PIF-induced elongation in low R:FR. *HFR1* was also not detected in the transcriptome of another wild species, *Rumex palustris*, which shows pronounced elongation when flooded, accompanied by transcriptional *KDR* induction (van Veen et al., 2013).

A second novel node of regulation identified here for SAS is that of RLKs. The THE1 and FER proteins regulate cell elongation (Lindner et al., 2012; Wolf and Höfte, 2014) but were not previously associated with photoreceptor responses. THE1 acts during cell expansion (Guo et al., 2009; Hématy et al., 2007) and is considered a cell wall integrity sensor, enhancing ROS production when cell wall integrity is lost (Denness et al., 2011). THE1 is redundant to HERK1 in regulating general vegetative growth (Guo et al., 2009). However, we show here that HERK1 plays no apparent role in SAS, whereas THE1 is a potent regulator independent of HERK1, as indicated by the single and double mutant data (Supplemental Figures 8A to 8C). In Arabidopsis, low R:FR light affected *THE1* expression in hypocotyls, possibly due to the presence of a PBE-box, a putative binding region for PIF1, PIF3, PIF4, and PIF5, in the *THE1* promoter (Oh et al., 2012; Pfeiffer et al., 2014; Martín et al., 2016). We show that this induction depends on PIF7, positioning *THE1* expression downstream of PIF7. Mutation of *the1* had no effect on the expression of the shade marker genes, suggesting that THE1 might act in an independent branch of the PIF7-controlled pathways, possibly acting at the cell wall during low R:FR-induced cell expansion that drives hypocotyl elongation. Low R:FR-induced elongation requires cell wall modification (Sasidharan et al., 2014, 2011) and we speculate that released polysaccharides from the reorganizing cell wall could act as ligands to activate THE1 (Lindner et al., 2012).

FER regulates female fertility through rupture of the growing pollen tube (Escobar-Restrepo et al., 2007; Duan et al., 2014) but has also been associated with vegetative growth (Guo et al., 2009; Li et al., 2015). Although *FER* expression is low R:FR-inducible in the two *Geranium* species, its expression in Arabidopsis is unaffected by low R:FR. The *fer* and *llg1* mutant data, nevertheless, indicate an important role of this receptor complex in shade avoidance of Arabidopsis hypocotyls, and the loss of *ATHB2* induction in *fer-5* shows that FER is somehow connected to part of the canonical SAS-associated gene expression network in Arabidopsis.

Our data suggest a specific role for these RLKs in low R:FR light-mediated elongation. Auxin levels are typically enhanced in low R:FR conditions (de Wit et al., 2015; Zheng et al., 2016; Tao et al., 2008; Keuskamp et al., 2010), and this is a key route to shoot elongation. However, IAA-induced hypocotyl elongation was not disturbed in any of the studied RLK mutants nor was *IAA19* expression affected in *the1-1* and *fer-5*, suggesting that the identified RLKs are not in the established shade avoidance control module of PIF-mediated auxin synthesis and response. How the phytochrome pathway regulates these RLKs, which putative ligands are controlling their activity in shade avoidance and which factors might be the kinase targets are all topics that future studies should elucidate.

Interestingly, FER has been directly associated with plant immunity (Kessler et al., 2010; Masachis et al., 2016) and *THE1* can regulate pathogen defense-related genes (Hématy et al., 2007). It remains to be determined if these factors also mediate shade avoidance–defense crosstalk.

In conclusion, our study using wild plants with different evolutionary histories has identified novel regulators of shade avoidance that had not been identified in Arabidopsis. The studies in Arabidopsis support the importance of these genes in SAS expression, but also hint that different organs and/or life cycle stages might express different modes of regulation. This study also shows that different species regulate the same components in different ways, consistent with differential control of shade avoidance.

METHODS

Plant Material and Growth Conditions

Geranium pyrenaicum (Cruydt-hoeck, Nijeberkoop, The Netherlands) and *Geranium robertianum* (Ecoflora, Halle, Belgium) seeds were germinated on polyethylene beads and water for 6 and 11 d, respectively, at saturated relative humidity, 20°C, under long-day conditions (16 h day, 8 h night; 180 μmol m^{-2} s^{-1} PAR; R:FR = 1.8). Seedlings were transferred to 70-mL pots with potting soil (mix Z2254; Primasta) and grown for two more weeks in long-day conditions (20°C; 70% relative humidity).

Different *Arabidopsis thaliana* genotypes (Col-0 and *pif7* [Leivar et al., 2008], *pif4 pif5* [Lorrain et al., 2008], *pif4 pif5 pif7* [de Wit et al., 2015], *the1-1* and *THE1*ox [Hématy et al., 2007], *the1-4*, *herk1*, and *herk1 the1* [Guo et al., 2009], *kdr-1* [SALK_048383C, Supplemental Figure 7A], *kdr-2* [SALK_033495C, Supplemental Figure 7A], *KDR-D* [Hyun and Lee, 2006; Supplemental Figure 7B], *fer-5* [SALK_029056C], *fer-4*, and *llg1-2* [Li et al., 2015]) were grown as previously described (de Wit et al., 2012), with a 9-h-light (180 μmol m^{-2} s^{-1} PAR)/15-h-dark photoperiod until ready for experiments at 4 weeks. For seedling experiments, seeds of the same Arabidopsis genotypes were surface-sterilized with chlorine gas, stratified (4 d dark, 4°C), and germinated on 0.5 Murashige and Skoog agar (0.8% v/w) plates with MES buffer (1 g/L). Germination was started with a 2-h light pulse, followed by 24 h darkness, and plates were then transferred to a long-day photoperiod as above. Treatments started 48 h after the light pulse.

Light Treatments

Low R:FR light conditions were obtained by supplementing standard growth chamber light (R:FR = 1.8; Philips HPI) with far-red LEDs (730-nm peak; Philips Greenpower Research modules), to obtain a R:FR of 0.2 without changing PAR. Blue light-depleted (± 4 μmol m^{-2} s^{-1}) conditions were obtained by filtering higher intensity white light using a Lee Medium Yellow 010 filter, to similar PAR as in controls (180 μmol m^{-2} s^{-1} for rosette plants, 110 μmol m^{-2} s^{-1} for seedlings). Light spectra are presented in Supplemental Figure 10. Treatments started at 10:00 AM.

Growth Measurements

Geranium and Arabidopsis petiole elongation was measured over a set period with a digital caliper (t_x - t_0). In *Geranium*, petiole growth rate kinetics were monitored using linear variable displacement transducers (type ST 200; Schlumberger Industries; Pierik et al., 2011; Voesenek et al., 2003). The linear variable displacement transducer was attached to the lamina-leaf junction of the second leaf 18 h prior to the start of the light treatment.

In Arabidopsis, hypocotyl length was measured at the end of a 4-d treatment using digital (600 dpi) images and ImageJ.

Statistical Analysis

Growth and bioassay data were analyzed by two-way ANOVA preceded by Levene's test to verify equal variances ($P > 0.05$), followed by a post-hoc Tukey test. Arabidopsis gene expression data were analyzed by a Student's *t* test preceded by an f-test to verify equal variances. If needed, data were ln transformed. All analyses were conducted in R and Microsoft Excel.

RNA Isolation and Gene Expression

For RT-qPCR, the apical 1 cm of the petiole of the second *Geranium* leaf of three individual plants (Figure 6; petiole elongation response) or the whole second leaf (petiole and lamina) of two individual plants (Figure 4C; pathogen defense of the leaf) were pooled as biological replicates. RNA was extracted using a Qiagen RNeasy kit with on-column DNaseI treatment. cDNA was synthesized using the Superscript III reverse transcriptase kit (Invitrogen) with RNase inhibitors and random primers. Quantitative RT-PCR was performed with SyberGreen Supermix (Bio-Rad) in a Viia7 PCR. The *Geranium* homolog of the PP2A subunit *PDF1* was used as a reference gene. Relative expression was calculated using the $2^{-\Delta\Delta Ct}$ method. Primers are listed in Supplemental Table 1. For Arabidopsis experiments in petioles, RNA was extracted from six pooled petioles (~5 mm) of three plants per biological replicate, after 4 h of light treatment. For Arabidopsis experiments in seedlings, 40 to 45 hypocotyls were harvested and pooled per biological replicate, after 24 h of light treatment. Extraction and analysis were similar as for the geraniums; the average Ct of *TUBULIN*, *APT1*, and *AT1G13320* (petioles), or the CT of *At1G13320* solely (hypocotyls), was used as a reference. Expression data of RLK-encoding genes from previously published experiments on Arabidopsis rosettes (heat map in Supplemental Figure 9) was obtained using the Genevestigator program and contains data from Leivar et al. (2012), Hornitschek et al. (2012), Tao et al. (2008), de Wit et al. (2013), Sessa et al. (2005), Ciolfi et al. (2013), Delker et al. (2010), Goda et al. (2008), Armstrong et al. (2004), and Okushima et al. (2005).

Illumina Sequencing and Bioinformatics

RNA was derived from the Geraniums as described. The replicates were a pool of 12 individual plants harvested in three separate experiments. The harvest time points were 2 and 11.5 h after the start of the far-red treatment (12:00 and 21:30, respectively). Normalized libraries for de novo assembly were constructed by Vertis Biotechnologie from pooled material of control, low R:FR, blue light-depleted, and green filter treated petioles and laminas, after 2, 11.5, and 24 h, for both species separately, using the kinetic denaturation-reassociation technique.

Illumina sequencing (paired-end, 101-bp reads) was performed by Macrogen, followed by de novo assembly (Trinity method; Grabherr et al., 2011) of the reference transcriptomes and alignment of the experimental transcripts (RSEM-based abundance estimation).

Putatively orthologous transcript groups within the two species were constructed using OrthoMCL clustering (as described in Li et al., 2003; Enright et al., 2002), with inflation factor 1.1 (for kingdom-wide OMCL, to increase the ability to detect putatively orthologous groups) or 3.0 (for expression analysis) and the similarity matrix of an all-versus-all discontiguous megaBLASTn of the two (or six) transcriptomes as input. The best BLAST hit with the Arabidopsis transcriptome was used to name *Geranium* OMCL groups.

For statistical analysis, read counts of all transcripts in an OMCL group were summed and a cutoff of minimally 20 reads in at least one treatment was applied to filter out low abundant families. To test for differentially expressed genes in single-factorial comparisons, a negative binomial model of OMCL group read numbers was made using the quantile-adjusted conditional maximum likelihood (qCML) method, followed by an exact test, including Benjamini and Hochberg's algorithm to control false discovery rates, of the EdgeR package (Bioconductor) (Robinson et al., 2010). The Cox-Reid profile-adjusted likelihood method in combination with a generalized linear model (likelihood ratio test [glmLRT]) of the EdgeR package was used in multifactor comparisons (McCarthy et al., 2012). A P value cutoff for differentially expressed genes was set at 0.01.

For GO analysis, differentially expressed *Geranium* OMCL groups, with a BLAST E-value $< 10^{-10}$ with Arabidopsis genes, were tested for GO term enrichment using the R package GOseq (Young et al., 2010), with correction for the total length of all transcripts in the *Geranium* OMCL group.

Pathogen Assays

Necrotrophic fungus *Botrytis cinerea* (strain B0510) was grown on half-strength potato dextrose agar (BD Difco) for 2 weeks before conidia were harvested in potato dextrose broth (BD Difco). *G. pyrenaicum* and *G. robertianum* seedlings (6 and 11 d after germination, respectively) were transferred to 19-mL pots with potting soil, and on the following day, a 2-μL droplet of 2.5×10^5 spores/mL of *B. cinerea* was applied to each cotyledon. Plants were kept at saturated relative humidity in a control white or low R:FR treatment. Lesion diameters were measured 3 d after inoculation.

Pharmacological Treatments

For the methyl-JA treatment, 30 min prior to the start of the light treatments, a solution of 100 μM methyl-JA or mock (0.1% ethanol) with 0.1% Tween 20 was sprayed on the plants. The IAA treatments of seedlings were performed as described previously (Keuskamp et al., 2011), with slight adjustments. Briefly, 200 μL of a concentrated, sterile IAA solution (600 μM) was applied to the plates to create a film on top of the agar, with a final concentration of 15 μM (0.1% DMSO).

Accession Numbers

Raw sequencing files and transcript shotgun assemblies (accession numbers HAGG01000001 to HAGG01168191 for *G. pyrenaicum*, and HAGH01000001 to HAGH01300137 for *G. robertianum*) are stored at the European Nucleotide Archive and combined under study accession number PRJEB18552 (http://www.ebi.ac.uk/ena/data/view/PRJEB18552). OMCL group assignment of the transcripts and RNA-seq expression data

are available in the ArrayExpress database (www.ebi.ac.uk/arrayexpress) under accession number E-MTAB-5371.

Supplemental Data

Supplemental Figure 1. A detailed analysis of low R:FR-induced growth over the time of day and in *Geranium* petioles.

Supplemental Figure 2. Low R:FR light suppresses petiole growth in *G. robertianum*, but not *G. pyrenaicum*, at a fixed time of the day.

Supplemental Figure 3. Gene Ontology analysis on low R:FR induced and repressed *Geranium* OMCL groups.

Supplemental Figure 4. Plant processes differentially regulated in low R:FR by the two *Geranium* species

Supplemental Figure 5. Low R:FR light affects MeJA-induced transcript abundance in *Geranium* and Arabidopsis, and pathogen infection does not affect *Geranium* growth in the shade.

Supplemental Figure 6. RT-qPCR on *Geranium* transcripts and validation of RNA sequencing.

Supplemental Figure 7. Confirmation of *kdr* mutants.

Supplemental Figure 8. HERK1 has no function in the Arabidopsis shade avoidance syndrome.

Supplemental Figure 9. *RLK* gene expression is hardly affected by low R:FR, *pif* mutations and IAA in previous transcriptome studies.

Supplemental Figure 10. Light spectra of the treatments used in this study.

Supplemental Table 1. Primer list.

ACKNOWLEDGMENTS

We thank Herman Höfte, Alice Cheung, Yanhai Yin, and Christian Fankhauser for kindly providing Arabidopsis seeds. We thank Saskia van Wees, Irene Vos, and Merel Steenbergen for providing *B. cinerea* strains and helping with the pathogen assays. Funding was provided by the Netherlands Organisation for Scientific Research to C.M.M.G. (no. 022.001.018) and R.P. (VIDI Grant 864.12.003).

AUTHOR CONTRIBUTIONS

C.M.M.G., R.P., and L.A.C.J.V. conceived the project. C.M.M.G., R.P., and D.H.K. designed the experiments. C.M.M.G., D.H.K., S.B., E.R., and I.T.K. performed the experiments. C.M.M.G. and H.v.V. analyzed the RNA-seq data. C.M.M.G. and R.P. wrote the manuscript.

Received October 17, 2016; revised January 10, 2017; accepted January 25, 2017; published January 30, 2017.

REFERENCES

Armstrong, J.I., Yuan, S., Dale, J.M., Tanner, V.N., and Theologis, A. (2004). Identification of inhibitors of auxin transcriptional activation by means of chemical genetics in Arabidopsis. Proc. Natl. Acad. Sci. USA **101:** 14978–14983.

Bai, M.-Y., Shang, J.-X., Oh, E., Fan, M., Bai, Y., Zentella, R., Sun, T.-P., and Wang, Z.-Y. (2012). Brassinosteroid, gibberellin and phytochrome impinge on a common transcription module in Arabidopsis. Nat. Cell Biol. **14:** 810–817.

Campos, M.L., Yoshida, Y., Major, I.T., de Oliveira Ferreira, D., Weraduwage, S.M., Froehlich, J.E., Johnson, B.F., Kramer, D.M., Jander, G., Sharkey, T.D., and Howe, G.A. (2016). Rewiring of jasmonate and phytochrome B signalling uncouples plant growth-defense tradeoffs. Nat. Commun. **7:** 12570.

Cargnel, M.D., Demkura, P.V., and Ballaré, C.L. (2014). Linking phytochrome to plant immunity: low red : far-red ratios increase Arabidopsis susceptibility to *Botrytis cinerea* by reducing the biosynthesis of indolic glucosinolates and camalexin. New Phytol. **204:** 342–354.

Carriedo, L.G., Maloof, J.N., and Brady, S.M. (2016). Molecular control of crop shade avoidance. Curr. Opin. Plant Biol. **30:** 151–158.

Cerrudo, I., Keller, M.M., Cargnel, M.D., Demkura, P.V., de Wit, M., Patitucci, M.S., Pierik, R., Pieterse, C.M.J., and Ballaré, C.L. (2012). Low red/far-red ratios reduce Arabidopsis resistance to *Botrytis cinerea* and jasmonate responses via a COI1-JAZ10-dependent, salicylic acid-independent mechanism. Plant Physiol. **158:** 2042–2052.

Chico, J.-M., Fernández-Barbero, G., Chini, A., Fernández-Calvo, P., Díez-Díaz, M., and Solano, R. (2014). Repression of jasmonate-dependent defenses by shade involves differential regulation of protein stability of MYC transcription factors and their JAZ repressors in Arabidopsis. Plant Cell **26:** 1967–1980.

Ciolfi, A., Sessa, G., Sassi, M., Possenti, M., Salvucci, S., Carabelli, M., Morelli, G., and Ruberti, I. (2013). Dynamics of the shade-avoidance response in Arabidopsis. Plant Physiol. **163:** 331–353.

Coluccio, M.P., Sanchez, S.E., Kasulin, L., Yanovsky, M.J., and Botto, J.F. (2011). Genetic mapping of natural variation in a shade avoidance response: ELF3 is the candidate gene for a QTL in hypocotyl growth regulation. J. Exp. Bot. **62:** 167–176.

Cortés, L.E., Weldegergis, B.T., Boccalandro, H.E., Dicke, M., and Ballar, C.L. (2016). Trading direct for indirect defense ? Phytochrome B inactivation in tomato attenuates direct anti-herbivore defenses whilst enhancing volatile-mediated attraction of predators. New Phytol. **212:** 1057–1071.

Das, D., St Onge, K.R., Voesenek, L.A.C.J., Pierik, R., and Sasidharan, R. (2016). Ethylene- and shade-induced hypocotyl elongation share transcriptome patterns and functional regulators. Plant Physiol. **172:** 718–733.

Delker, C., Pöschl, Y., Raschke, A., Ullrich, K., Ettingshausen, S., Hauptmann, V., Grosse, I., and Quint, M. (2010). Natural variation of transcriptional auxin response networks in *Arabidopsis thaliana*. Plant Cell **22:** 2184–2200.

de Lucas, M., Davière, J.-M., Rodríguez-Falcón, M., Pontin, M., Iglesias-Pedraz, J.M., Lorrain, S., Fankhauser, C., Blázquez, M.A., Titarenko, E., and Prat, S. (2008). A molecular framework for light and gibberellin control of cell elongation. Nature **451:** 480–484.

Denness, L., McKenna, J.F., Segonzac, C., Wormit, A., Madhou, P., Bennett, M., Mansfield, J., Zipfel, C., and Hamann, T. (2011). Cell wall damage-induced lignin biosynthesis is regulated by a reactive oxygen species- and jasmonic acid-dependent process in Arabidopsis. Plant Physiol. **156:** 1364–1374.

de Wit, M., Kegge, W., Evers, J.B., Vergeer-van Eijk, M.H., Gankema, P., Voesenek, L.A.C.J., and Pierik, R. (2012). Plant neighbor detection through touching leaf tips precedes phytochrome signals. Proc. Natl. Acad. Sci. USA **109:** 14705–14710.

de Wit, M., Ljung, K., and Fankhauser, C. (2015). Contrasting growth responses in lamina and petiole during neighbor detection depend on differential auxin responsiveness rather than different auxin levels. New Phytol. **208:** 198–209.

de Wit, M., Spoel, S.H., Sanchez-Perez, G.F., Gommers, C.M.M., Pieterse, C.M.J., Voesenek, L.A.C.J., and Pierik, R. (2013). Perception of low red:far-red ratio compromises both salicylic acid- and jasmonic acid-dependent pathogen defences in Arabidopsis. Plant J. **75:** 90–103.

Djakovic-Petrovic, T., de Wit, M., Voesenek, L.A.C.J., and Pierik, R. (2007). DELLA protein function in growth responses to canopy signals. Plant J. **51:** 117–126.

Duan, Q., Kita, D., Johnson, E.A., Aggarwal, M., Gates, L., Wu, H.-M., and Cheung, A.Y. (2014). Reactive oxygen species mediate pollen tube rupture to release sperm for fertilization in Arabidopsis. Nat. Commun. **5:** 3129.

Enright, A.J., Van Dongen, S., and Ouzounis, C.A. (2002). An efficient algorithm for large-scale detection of protein families. Nucleic Acids Res. **30:** 1575–1584.

Escobar-Restrepo, J.-M., Huck, N., Kessler, S., Gagliardini, V., Gheyselinck, J., Yang, W.-C., and Grossniklaus, U. (2007). The FERONIA receptor-like kinase mediates male-female interactions during pollen tube reception. Science **317:** 656–660.

Filiault, D.L., and Maloof, J.N. (2012). A genome-wide association study identifies variants underlying the *Arabidopsis thaliana* shade avoidance response. PLoS Genet. **8:** e1002589.

Fraser, D.P., Hayes, S., and Franklin, K.A. (2016). Photoreceptor crosstalk in shade avoidance. Curr. Opin. Plant Biol. **33:** 1–7.

Gilbert, I.R., Jarvis, P.G., and Smith, H. (2001). Proximity signal and shade avoidance differences between early and late successional trees. Nature **411:** 792–795.

Goda, H., et al. (2008). The AtGenExpress hormone and chemical treatment data set: experimental design, data evaluation, model data analysis and data access. Plant J. **55:** 526–542.

Gommers, C.M.M., Visser, E.J.W., St Onge, K.R., Voesenek, L.A.C.J., and Pierik, R. (2013). Shade tolerance: when growing tall is not an option. Trends Plant Sci. **18:** 65–71.

Grabherr, M.G., et al. (2011). Full-length transcriptome assembly from RNA-Seq data without a reference genome. Nat. Biotechnol. **29:** 644–652.

Guo, H., Li, L., Ye, H., Yu, X., Algreen, A., and Yin, Y. (2009). Three related receptor-like kinases are required for optimal cell elongation in *Arabidopsis thaliana*. Proc. Natl. Acad. Sci. USA **106:** 7648–7653.

Hématy, K., Sado, P.-E., Van Tuinen, A., Rochange, S., Desnos, T., Balzergue, S., Pelletier, S., Renou, J.-P., and Höfte, H. (2007). A receptor-like kinase mediates the response of Arabidopsis cells to the inhibition of cellulose synthesis. Curr. Biol. **17:** 922–931.

Hong, S.-Y., Seo, P.J., Ryu, J.Y., Cho, S.-H., Woo, J.-C., and Park, C.-M. (2013). A competitive peptide inhibitor KIDARI negatively regulates HFR1 by forming nonfunctional heterodimers in Arabidopsis photomorphogenesis. Mol. Cells **35:** 25–31.

Hornitschek, P., Kohnen, M.V., Lorrain, S., Rougemont, J., Ljung, K., López-Vidriero, I., Franco-Zorrilla, J.M., Solano, R., Trevisan, M., Pradervand, S., Xenarios, I., and Fankhauser, C. (2012). Phytochrome interacting factors 4 and 5 control seedling growth in changing light conditions by directly controlling auxin signaling. Plant J. **71:** 699–711.

Hornitschek, P., Lorrain, S., Zoete, V., Michielin, O., and Fankhauser, C. (2009). Inhibition of the shade avoidance response by formation of non-DNA binding bHLH heterodimers. EMBO J. **28:** 3893–3902.

Hyun, Y., and Lee, I. (2006). KIDARI, encoding a non-DNA Binding bHLH protein, represses light signal transduction in *Arabidopsis thaliana*. Plant Mol. Biol. **61:** 283–296.

Izaguirre, M.M., Mazza, C.A., Biondini, M., Baldwin, I.T., and Ballaré, C.L. (2006). Remote sensing of future competitors: impacts on plant defenses. Proc. Natl. Acad. Sci. USA **103:** 7170–7174.

Jiménez-Gómez, J.M., Wallace, A.D., and Maloof, J.N. (2010). Network analysis identifies ELF3 as a QTL for the shade avoidance response in Arabidopsis. PLoS Genet. **6:** e1001100.

Kessler, S.A., Shimosato-Asano, H., Keinath, N.F., Wuest, S.E., Ingram, G., Panstruga, R., and Grossniklaus, U. (2010). Conserved molecular components for pollen tube reception and fungal invasion. Science **330:** 968–971.

Keuskamp, D.H., Pollmann, S., Voesenek, L.A.C.J., Peeters, A.J.M., and Pierik, R. (2010). Auxin transport through PIN-FORMED 3 (PIN3) controls shade avoidance and fitness during competition. Proc. Natl. Acad. Sci. USA **107:** 22740–22744.

Keuskamp, D.H., Sasidharan, R., Vos, I., Peeters, A.J.M., Voesenek, L.A.C.J., and Pierik, R. (2011). Blue-light-mediated shade avoidance requires combined auxin and brassinosteroid action in Arabidopsis seedlings. Plant J. **67:** 208–217.

Kohnen, M.V., Schmid-Siegert, E., Trevisan, M., Petrolati, L.A., Sénéchal, F., Müller-Moulé, P., Maloof, J., Xenarios, I., and Fankhauser, C. (2016). Neighbor detection induces organ-specific transcriptomes, revealing patterns underlying hypocotyl-specific frowth. Plant Cell **28:** 2889–2904.

Leivar, P., Monte, E., Al-Sady, B., Carle, C., Storer, A., Alonso, J.M., Ecker, J.R., and Quail, P.H. (2008). The Arabidopsis phytochrome-interacting factor PIF7, together with PIF3 and PIF4, regulates responses to prolonged red light by modulating phyB levels. Plant Cell **20:** 337–352.

Leivar, P., Tepperman, J.M., Cohn, M.M., Monte, E., Al-Sady, B., Erickson, E., and Quail, P.H. (2012). Dynamic antagonism between phytochromes and PIF family basic helix-loop-helix factors induces selective reciprocal responses to light and shade in a rapidly responsive transcriptional network in Arabidopsis. Plant Cell **24:** 1398–1419.

Li, C., et al. (2015). Glycosylphosphatidylinositol-anchored proteins as chaperones and co-receptors for FERONIA receptor kinase signaling in Arabidopsis. eLife **4:** 1–21.

Li, L., et al. (2012). Linking photoreceptor excitation to changes in plant architecture. Genes Dev. **26:** 785–790.

Li, L., Stoeckert, C.J., Jr., and Roos, D.S. (2003). OrthoMCL: identification of ortholog groups for eukaryotic genomes. Genome Res. **13:** 2178–2189.

Lindner, H., Müller, L.M., Boisson-Dernier, A., and Grossniklaus, U. (2012). CrRLK1L receptor-like kinases: not just another brick in the wall. Curr. Opin. Plant Biol. **15:** 659–669.

Lorrain, S., Allen, T., Duek, P.D., Whitelam, G.C., and Fankhauser, C. (2008). Phytochrome-mediated inhibition of shade avoidance involves degradation of growth-promoting bHLH transcription factors. Plant J. **53:** 312–323.

Martín, G., Leivar, P., Ludevid, D., Tepperman, J.M., Quail, P.H., and Monte, E. (2016). Phytochrome and retrograde signalling pathways converge to antagonistically regulate a light-induced transcriptional network. Nat. Commun. **7:** 11431.

Masachis, S., Segorbe, D., Turrà, D., Leon-Ruiz, M., Fürst, U., El Ghalid, M., Leonard, G., López-Berges, M.S., Richards, T.A., Felix, G., and Di Pietro, A. (2016). A fungal pathogen secretes plant alkalinizing peptides to increase infection. Nat. Microbiol. **1:** 16043.

McCarthy, D.J., Chen, Y., and Smyth, G.K. (2012). Differential expression analysis of multifactor RNA-Seq experiments with respect to biological variation. Nucleic Acids Res. **40:** 4288–4297.

Moreno, J.E., Tao, Y., Chory, J., and Ballaré, C.L. (2009). Ecological modulation of plant defense via phytochrome control of jasmonate sensitivity. Proc. Natl. Acad. Sci. USA **106:** 4935–4940.

Morgan, D.C., and Smith, H. (1978). The relationship between phytochrome-photoequilibrium and development in light grown *Chenopodium album* L. Planta **142:** 187–193.

Nozue, K., Tat, A.V., Kumar Devisetty, U., Robinson, M., Mumbach, M.R., Ichihashi, Y., Lekkala, S., and Maloof, J.N. (2015). Shade avoidance components and pathways in adult plants revealed by phenotypic profiling. PLoS Genet. **11:** e1004953.

Oh, E., Zhu, J.-Y., and Wang, Z.-Y. (2012). Interaction between BZR1 and PIF4 integrates brassinosteroid and environmental responses. Nat. Cell Biol. **14:** 802–809.

Okushima, Y., et al. (2005). Functional genomic analysis of the AUXIN RESPONSE FACTOR gene family members in *Arabidopsis thaliana*: unique and overlapping functions of ARF7 and ARF19. Plant Cell **17:** 444–463.

Pfeiffer, A., Shi, H., Tepperman, J.M., Zhang, Y., and Quail, P.H. (2014). Combinatorial complexity in a transcriptionally centered signaling hub in Arabidopsis. Mol. Plant **7:** 1598–1618.

Pierik, R., and Testerink, C. (2014). The art of being flexible: how to escape from shade, salt, and drought. Plant Physiol. **166:** 5–22.

Pierik, R., De Wit, M., and Voesenek, L.A. (2011). Growth-mediated stress escape: convergence of signal transduction pathways activated upon exposure to two different environmental stresses. New Phytol. **189:** 122–134.

Quail, P.H. (2002). Phytochrome photosensory signalling networks. Nat. Rev. Mol. Cell Biol. **3:** 85–93.

Robinson, M.D., McCarthy, D.J., and Smyth, G.K. (2010). edgeR: a Bioconductor package for differential expression analysis of digital gene expression data. Bioinformatics **26:** 139–140.

Sasidharan, R., Chinnappa, C.C., Voesenek, L.A.C.J., and Pierik, R. (2009). A molecular basis for the physiological variation in shade avoidance responses: a tale of two ecotypes. Plant Signal. Behav. **4:** 528–529.

Sasidharan, R., Keuskamp, D.H., Kooke, R., Voesenek, L.A.C.J., and Pierik, R. (2014). Interactions between auxin, microtubules and XTHs mediate green shade- induced petiole elongation in Arabidopsis. PLoS One **9:** e90587.

Sasidharan, R., Voesenek, L.A., and Pierik, R. (2011). Cell wall modifying proteins mediate plant acclimatization to biotic and abiotic stresses. Crit. Rev. Plant Sci. **30:** 548–562.

Sessa, G., Carabelli, M., Sassi, M., Ciolfi, A., Possenti, M., Mittempergher, F., Becker, J., Morelli, G., and Ruberti, I. (2005). A dynamic balance between gene activation and repression regulates the shade avoidance response in Arabidopsis. Genes Dev. **19:** 2811–2815.

Tao, Y., et al. (2008). Rapid synthesis of auxin via a new tryptophan-dependent pathway is required for shade avoidance in plants. Cell **133:** 164–176.

Tofts, R.J. (2004). *Geranium robertianum* L. J. Ecol. **92:** 537–555.

Toledo-Ortiz, G., Huq, E., and Rodríguez-Concepción, M. (2010). Direct regulation of phytoene synthase gene expression and carotenoid biosynthesis by phytochrome-interacting factors. Proc. Natl. Acad. Sci. USA **107:** 11626–11631.

Valladares, F., and Niinemets, Ü. (2008). Shade tolerance, a key plant feature of complex nature and consequences. Annu. Rev. Ecol. Evol. Syst. **39:** 237–257.

van Veen, H., Mustroph, A., Barding, G.A., Vergeer-van Eijk, M., Welschen-Evertman, R.A.M., Pedersen, O., Visser, E.J.W., Larive, C.K., Pierik, R., Bailey-Serres, J., Voesenek, L.A.C.J., and Sasidharan, R. (2013). Two Rumex species from contrasting hydrological niches regulate flooding tolerance through distinct mechanisms. Plant Cell **25:** 4691–4707.

Voesenek, L.A.C.J., Jackson, M.B., Toebes, A.H.W., Huibers, W., Vriezen, W.H., and Colmer, T.D. (2003). De-submergence-induced ethylene production in Rumex palustris: regulation and ecophysiological significance. Plant J. **33:** 341–352.

Warburg, A.E.F. (1938). Taxonomy and relationship in the Geraniales in the light of their cytology. New Phytol. **37:** 130–159.

Wolf, S., and Höfte, H. (2014). Growth control: a saga of cell walls, ROS, and peptide receptors. Plant Cell **26:** 1848–1856.

Yang, D., Seaton, D.D., Krahmer, J., and Halliday, K.J. (2016). Photoreceptor effects on plant biomass, resource allocation, and metabolic state. Proc. Natl. Acad. Sci. USA **113:** 7667–7672.

Young, M.D., Wakefield, M.J., Smyth, G.K., and Oshlack, A. (2010). Gene ontology analysis for RNA-seq: accounting for selection bias. Genome Biol. **11:** R14.

Zheng, Z., Guo, Y., Chen, W., Ljung, K., Noel, J.P., and Chory, J. (2016). Local auxin metabolism regulates environment-induced hypocotyl elongation. Nat. Plants **2:** 1–9.